Photocatalytic Water Oxidation in a Buffered Tris(2,2′-bipyridyl)ruthenium Complex-Colloidal IrO_2 System

Michikazu Hara, Chad C. Waraksa, John T. Lean, Bradley A. Lewis, and Thomas E. Mallouk*

Department of Chemistry, The Pennsylvania University, University Park, Pennsylvania 16802

Received: January 27, 2000; In Final Form: March 23, 2000

A buffered tris(2,2′-bipyridyl)ruthenium complex-colloidal IrO_2 system was studied as a photocatalyst for the production of O_2 from water. Phosphate buffer, which has historically been used to control the pH in this system, accelerates the decomposition of the photosensitizer and inhibits O_2 evolution, whereas sodium hexafluorosilicate (Na_2SiF_6)−base solutions are ideal buffers for the reaction. Na_2SiF_6-containing buffers poise the solution under visible light irradiation at ca. pH 5, preventing the pH drop that accompanies oxidation of water in unbuffered solutions. Decomposition of the photosensitizer is not kinetically competitive with oxygen evolution in these buffers. In particular, the Na_2SiF_6−$NaHCO_3$ buffer greatly improves the turnover number of the photosensitizer, relative to previously used phosphate buffers, without any decrease in activity. Photocatalytic reactions studied under various conditions suggest that adsorbed carbonate or bicarbonate on the surface of the colloidal IrO_2 particles contributes to the increased turnover number of the photosensitizer.

Introduction

Considerable research effort has gone into the design and study of photosystems for the cyclic cleavage of water into H_2 and O_2.[1−3] Any such system that could work under visible light irradiation would have genuine applications in solar energy conversion and storage. However, no satisfactory system has been devised to date. One of the biggest stumbling blocks preventing the construction of an overall photosystem is the absence of a highly effective and selective O_2 evolving system. As a four-electron redox process, the evolution of O_2 from water is more difficult than kinetically simpler processes, such as H_2 evolution. While there has been encouraging recent progress on the design of molecular catalysts for the four-electron oxidation of water, to date none of these compounds work near the formal potential of the oxygen/water couple.[4]

It is well known that tris(2,2′-bipyridyl)ruthenium(III) ($[Ru(bpy)_3]^{3+}$) and its derivatives are capable of oxidizing water to O_2 at the surface of colloidal and bulk heterogeneous catalysts.[5−9] A photocatalytic cycle for such a system is shown in Scheme 1. In this scheme, visible light is absorbed by $[Ru(bpy)_3]^{2+}$, and the MLCT state of the sensitizer ($[Ru(bpy)_3]^{2+*}$) is formed. The latter is oxidized to $[Ru(bpy)_3]^{3+}$ by an appropriate sacrificial acceptor such as $S_2O_8^{2-}$. Without a homogeneous or heterogeneous oxygen evolution catalyst, no O_2 is formed and $[Ru(bpy)_3]^{3+}$ decomposes rapidly, even though the sacrificial acceptor is irreversibly reduced. In the presence of catalysts such as RuO_2 and IrO_2, the photosensitizer can be recycled and O_2 is detected as a reaction product. This reaction proceeds efficiently at ca. pH 5, but the rate decreases above and below this pH. The initial quantum efficiency for O_2 evolution in this system reaches 40−60% under optimized conditions.[7,9] The photosensitizer, however, has a short lifetime, and its turnover number does not exceed 80, even under the most optimized conditions.[7] This can be attributed to decomposition of the photosensitizer, which is kinetically competitive with the oxidation of water.[10] The poor stability of the photosensitizer remains the most serious obstacle to developing a suitable anodic branch of a nanostuctured water splitting photosystem.[11]

SCHEME 1. Schematic of the Photocatalytic Oxidation of Water by the $[Ru(bpy)_3]^{2+}$−Catalyst System, Showing the Competing Decomposition Reaction of the Oxidized Sensitizer

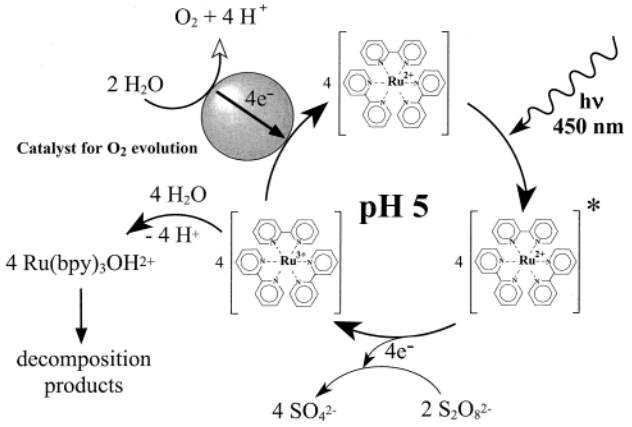

There are several advantages to using colloids rather than bulk powders for photocatalysis. Kinetic measurements are more easily performed by standard transmission UV−visible spectroscopy because the size of the particles is much smaller than the wavelength of light. The most important advantage is that charged colloidal particles can more easily be incorporated into photosynthetic assemblies based on zeolites or layer-by-layer assemblies of oppositely charged macromolecules.[11−14] Among transition metal oxide colloids, the oxides of Ru and Ir have been most extensively studied. While RuO_2 colloids are effective catalysts for O_2 evolution under photochemical conditions, they undergo anodic corrosion when treated with strong oxidizing agents.[7] Bulk IrO_2 powder and colloidal $IrO_2 \cdot xH_2O$ have been found to be more stable for water oxidation than RuO_2, and they also have high catalytic activities for O_2 evolution.[8,9]

10.1021/jp000321x CCC: $19.00
Published on Web 05/09/2000

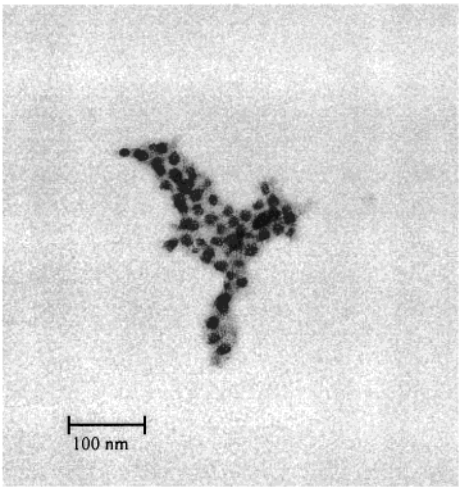

Figure 1. TEM images of colloidal IrO_2 particles.

In this paper, we describe the photocatalytic oxidation of water, using the well-studied $[Ru(bpy)_3]^{2+}-IrO_2 \cdot xH_2O$ colloid $-S_2O_8^{2-}$ system in various buffers. We find that the turnover number and decomposition rate of the photosensitizer under photochemical conditions are strongly dependent on the composition of the buffer. Conventional phosphate−borate buffers accelerate the decomposition of the photosensitizer. On the other hand, Na_2SiF_6−base buffers improve turnover number, and the photosensitizer has an especially long lifetime in Na_2SiF_6−$NaHCO_3$ buffers.

Experimental Section

Materials. Reagent grade KH_2PO_4, $Na_2B_4O_7 \cdot 10H_2O$, Na_2SiF_6, $NaHCO_3$, $Na_2S_2O_8$, Na_2SO_4, and sodium hydrogen citrate sesquihydrate, $NaO_2CCH_2C(OH)(CO_2H)CH_2CO_2Na \cdot 1.5H_2O$, were obtained form commercial sources. $[Ru(bpy)_3]Cl_2 \cdot 6H_2O$ and potassium hexachloroiridate, K_2IrCl_6, were used as received from Aldrich and Alfa, respectively.

Preparation of $IrO_2 \cdot xH_2O$ Colloid. $IrO_2 \cdot xH_2O$ colloid was prepared by hydrolysis of hexachloroiridate ($IrCl_6^{2-}$) in the presence of citrate ions as a stabilizer.[8] K_2IrCl_6 (0.030 g, 6.2×10^{-5} mol) was added to an aqueous solution of 0.05 g of sodium hydrogen citrate sesquihydrate (1.9×10^{-4} mol), which was dissolved in 50 mL of deionized water. The red−brown solution was adjusted to pH 7.5 with 0.25 M NaOH solution and was heated to 95 °C in an oil bath with constant stirring. After heating for 30 min, the solution was cooled to room temperature and the NaOH solution was added to adjust the pH to 7.5. The addition of NaOH solution at room temperature, followed by heating at 95 °C for 30 min was repeated until the pH had stabilized at 7.5. The solution was transferred to a round-bottom flask with a reflux condenser and was kept at 95 °C for 2 h with oxygen bubbling through the solution. The solution became deep blue, signaling the formation of colloidal $IrO_2 \cdot xH_2O$, toward the end of the reaction.[8] The colloidal solution was cooled to room temperature before being stirred with 10 mL of moderate anion-exchange resin, DOWEX 2X8-50, to remove excess citrate ions. After 30 min, the resin was removed by filtration and the final solution diluted to 100 mL. Figure 1 shows TEM images of colloidal IrO_2 obtained in this way. The diameter of the colloidal particles was estimated to be 10−20 nm. The citrate-stabilized colloid was stable over a period of three months.

Photocatalytic Oxidation of Water. The reaction was carried out in 5 mL aqueous solutions containing $[Ru(bpy)_3]Cl_2 \cdot 6H_2O$, colloidal IrO_2, $Na_2S_2O_8$, Na_2SO_4, and buffer in a Pyrex test tube reactor (36.5 mL). The reactor was sealed with a silicone rubber septum, and was put in an outer Pyrex vessel with a rubber septum into which Ar flowed to prevent contamination of the reactor by the atmosphere. The concentrations of colloidal IrO_2, $Na_2S_2O_8$, and Na_2SO_4 in the solution were 6.2×10^{-5}, 1.0×10^{-2}, and 5.0×10^{-2} M, respectively, while the concentrations of $[Ru(bpy)_3]^{2+}$ and buffer were varied (see below). KH_2PO_4−$Na_2B_4O_7$, Na_2SiF_6−$Na_2B_4O_7$, and Na_2SiF_6−$NaHCO_3$ solutions were used as buffers, and the solution was adjusted to pH 4.5−5.8 by these buffers before the photochemical reaction. To remove O_2 from the reactor, Ar gas was bubbled through the solution in the dark by means of two needles that penetrated the rubber septa of the reactor and the Pyrex vessel. After 30 min, the constantly stirred solutions were irradiated with a Xe lamp of 300 W, equipped with a 450 ± 20 nm interference filter. The intensity of visible light impinging on the sample was typically 18 mW/cm^2. The evolved gas that accumulated in the dead volume of the reactor was withdrawn by a sample-lock syringe and was analyzed by gas chromatography (GC) using a thermal conductivity detector and room-temperature molecular sieve 5A columns, which were purchased from Supelco. There was no detectable contamination due to air, judging by the absence of a GC peak for nitrogen, during the reactions.

Determination of $[Ru(bpy)_3]^{2+}$ and $[Ru(bpy)_3]^{3+}$ Concentrations under Photochemical Conditions. The time course of the concentrations of $[Ru(bpy)_3]^{2+}$ and $[Ru(bpy)_3]^{3+}$ was measured under photochemical conditions to estimate the rate constant of decomposition of the oxidized photosensitizer. The reaction was carried out in solutions without colloidal IrO_2. Other conditions were the same as those described above. $[Ru(bpy)_3]^{3+}$ produced by reduction of the sacrificial acceptor does not return to $[Ru(bpy)_3]^{2+}$ under these conditions. The reaction system was placed in the light path of an HP 8452A diode array UV−vis spectrometer and was irradiated with visible light at right angles. The concentration of $[Ru(bpy)_3]^{2+}$ was measured by monitoring the MLCT absorption bands in the range of 400 to 500 nm. The concentration of $[Ru(bpy)_3]^{3+}$ was not measured directly because $[Ru(bpy)_3]^{3+}$ absorbs weakly in the visible. After set intervals of irradiation, 0.1 mL methanol was added to the solution in the dark, and photochemically generated $[Ru(bpy)_3]^{3+}$ was reduced to $[Ru(bpy)_3]^{2+}$. The concentration of $[Ru(bpy)_3]^{3+}$ under photochemical conditions could therefore be estimated by determining the amount of $[Ru(bpy)_3]^{2+}$ recovered from $[Ru(bpy)_3]^{3+}$. The amount of $[Ru(bpy)_3]^{3+}$ that had decomposed in the same time interval could likewise be calculated by difference.

Results and Discussion

Oxygen Evolution and Decomposition of $[Ru(bpy)_3]^{3+}$ in Phosphate−Borate Buffers. Figure 2 shows time courses of O_2 evolution and turnover number with respect to the photosensitizer under photochemical conditions in conventional KH_2PO_4−$Na_2B_4O_7$ buffers. The concentration of $[Ru(bpy)_3]^{2+}$ was 1.1×10^{-4} M, and the KH_2PO_4:$Na_2B_4O_7$ mole ratio in the buffer was 1.00:0.04. The pH before and after the reaction are indicated at the end of each curve in Figure 2. In each case, the amount of evolved O_2 levels off when the photosensitizer is completely decomposed.

Figure 3 correlates the total turnover number to the concentration of the KH_2PO_4−$Na_2B_4O_7$ buffer. In the case of no buffer, the rate of O_2 evolution was slow, and the total turnover number did not reach even 10. During the course of this reaction, the

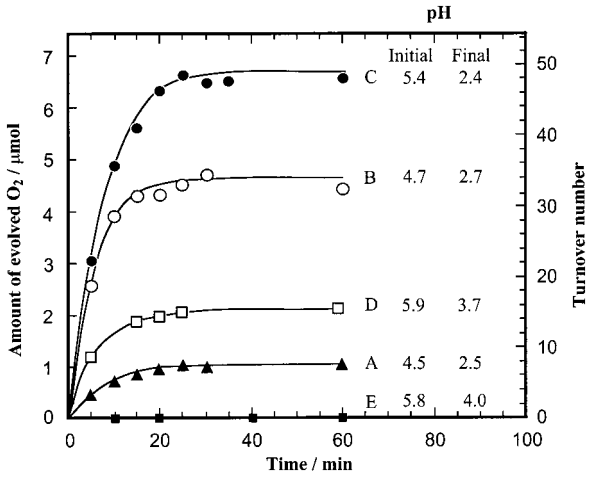

Figure 2. Time course of O_2 evolution from $[Ru(bpy)_3]^{2+}$−colloidal IrO_2−persulfate system in KH_2PO_4−$Na_2B_4O_7$ buffer. $[Ru(bpy)_3]^{2+}$: 1.1×10^{-4} M. Colloidal IrO_2: 6.2×10^{-4} M. $Na_2S_2O_8$: 1.0×10^{-4} M. KH_2PO_4:$Na_2B_4O_7$ = 1.00:0.04, $\lambda = 450 \pm 20$ nm. (A) no buffer, (B) 1.9×10^{-3} M buffer, (C) 1.1×10^{-2} M buffer, (D) 3.6×10^{-2} M buffer, (E) 7.5×10^{-2} M buffer.

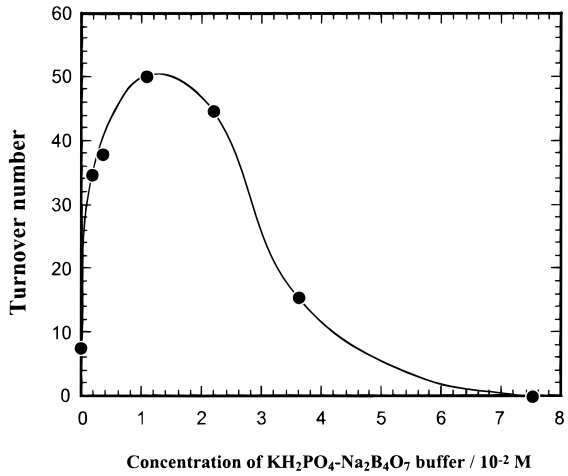

Figure 3. Dependence of the turnover number of the photosensitizer on the concentration of KH_2PO_4−$Na_2B_4O_7$ buffer.

pH fell, owing to the formation of protons in the oxidation of water. O_2 evolution from the $[Ru(bpy)_3]^{2+}$−IrO_2−$S_2O_8^{2-}$ system is known to proceed most efficiently at ca. pH 5.[7] The decomposition of $[Ru(bpy)_3]^{3+}$, which involves OH^- attack on the bipyridine ring,[10] is accelerated at higher pH. At lower pH the decomposition reaction proceeds in preference to O_2 evolution because the latter becomes thermodynamically less favorable and therefore slower. When KH_2PO_4−$Na_2B_4O_7$ buffer was added to the solution, the rate of O_2 evolution and turnover number increased with increasing buffer concentration, reaching a maximum at 1.1×10^{-2} M. However, beyond this point, addition of buffer reduced both the rate of O_2 evolution and the turnover number. At the highest buffer concentration shown, 7.5×10^{-2} M, O_2 was not evolved in measurable amounts. In all reactions, colloidal IrO_2 was not precipitated during reaction and there was no noticeable difference in TEM images of colloidal IrO_2 before and after reaction. The yellow color of $[Ru(bpy)_3]^{2+}$ faded from the solution after 10−15 min reaction at 1.9×10^{-3} to 3.6×10^{-2} M buffer, whereas in the most concentrated buffer solutions the color disappeared within 5 min. These results indicate that the photosensitizer is subject to accelerated decomposition in concentrated KH_2PO_4−$Na_2B_4O_7$ buffer solutions.

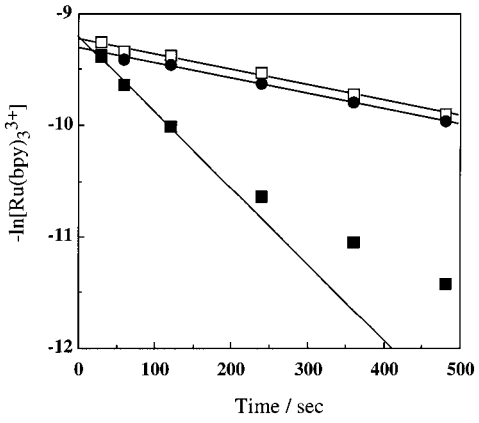

Figure 4. Time course of the logarithm of concentration of $[Ru(bpy)_3]^{3+}$, detected as $[Ru(bpy)_3]^{2+}$ by addition of methanol after irradiation, in KH_2PO_4−$Na_2B_4O_7$ buffers without colloidal IrO_2. Open squares: without buffer. Filled circles: in 1.1×10^{-2} M buffer. Filled squares: in 7.5×10^{-2} M buffer.

TABLE 1. Decomposition Rate Constant of $[Ru(bpy)_3]^{3+}$ in Various Buffers

buffer	mole ratio	concentration/M	k_d/s^{-1}
none			1.4×10^{-3}
KH_2PO_4−$Na_2B_4O_7$	(1.00:0.04)	1.1×10^{-2}	1.4×10^{-3}
		7.5×10^{-2}	6.7×10^{-3}
Na_2SiF_6−$Na_2B_4O_7$	(1.0:4.3)	1.4×10^{-2}	1.4×10^{-3}
Na_2SiF_6−$NaHCO_3$	(1.0:1.3)	5.0×10^{-2}	1.6×10^{-3}

Figure 4 shows time courses of the concentration of $[Ru(bpy)_3]^{3+}$ under photochemical conditions without colloidal IrO_2 in KH_2PO_4−$Na_2B_4O_7$ buffer. The $[Ru(bpy)_3]^{2+}$ concentration (not shown) decreases to near zero levels within 30 s under irradiation because $[Ru(bpy)_3]^{2+*}$ is rapidly oxidized by $S_2O_8^{2-}$.[5-7] The $[Ru(bpy)_3]^{3+}$ concentration increases rapidly in the same early stage of the reaction, but then decreases because of irreversible decomposition. There was no significant difference in the time course of $[Ru(bpy)_3]^{3+}$ concentrations between no buffer and 1.1×10^{-2} M buffer. In both cases, the decay kinetics are first-order and the rate constant k_d (see Table 1) was 1.4×10^{-3} s^{-1}. In the case of 7.5×10^{-2} M buffer, the kinetics are more complex, but the initial rate of decomposition of $[Ru(bpy)_3]^{3+}$ was much faster ($k_d = 6.7 \times 10^{-3}$ s^{-1}) and the complex was largely decomposed after 2 min. Apparently, concentrated KH_2PO_4−$Na_2B_4O_7$ greatly accelerates the decomposition of $[Ru(bpy)_3]^{3+}$.

To determine which of the two components in this buffer is responsible for decomposition of the photosensitizer, the rates were measured separately in 7.2×10^{-2} M KH_2PO_4 and 2.9×10^{-3} M $Na_2B_4O_7$ solutions, which corresponded to the individual concentrations in the 7.5×10^{-2} M KH_2PO_4−$Na_2B_4O_7$ buffer. The KH_2PO_4 and $Na_2B_4O_7$ solutions were adjusted to pH 5.5 by addition of NaOH and HCl solutions, respectively. In the case of $Na_2B_4O_7$, k_d was 1.5×10^{-3} s^{-1} as in the unbuffered and 1.1×10^{-2} M KH_2PO_4−$Na_2B_4O_7$ buffer solutions. On the other hand, k_d in KH_2PO_4 solution was comparable to that in 7.5×10^{-2} M KH_2PO_4−$Na_2B_4O_7$, confirming that phosphate accelerates the decomposition of $[Ru(bpy)_3]^{3+}$.

The accepted mechanism for decomposition of $[Ru(bpy)_3]^{3+}$ in water involves nucleophilic attack of water on the bpy ring, either in the ground state or excited state of the complex (see Scheme 1), to form a bpyOH ligand.[10] Because phosphate is a relatively weak nucleophile, it is difficult to understand why it should accelerate the reaction to a much greater extent than other oxyanions (borate, bicarbonate) tested. Even in the absence of phosphate, the overall decomposition pathway is quite complex

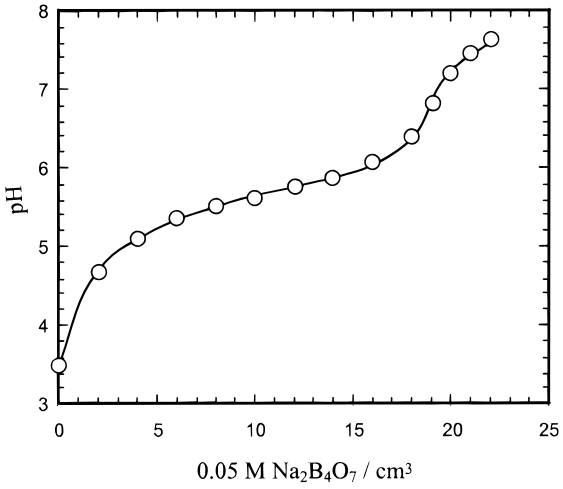

Figure 5. Titration curve of Na_2SiF_6 with $Na_2B_4O_7$ solution. Na_2SiF_6: 2.6×10^{-2} M, 40 mL. $Na_2B_4O_7$ solution: 5.0×10^{-2} M.

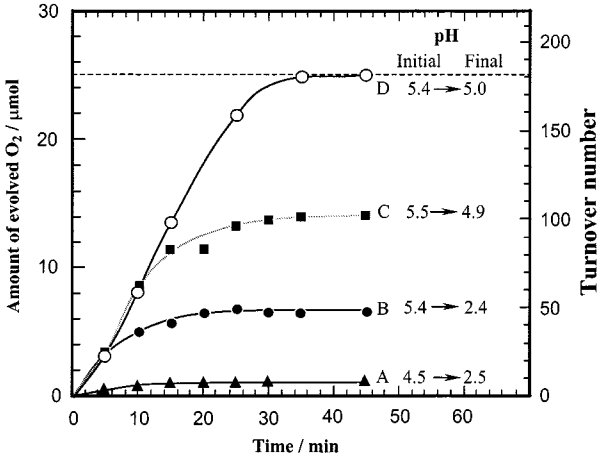

Figure 6. Time course of photochemical O_2 evolution and turnover number in various buffers. (A) No buffer, (B) 1.1×10^{-2} M (mole ratio 1.00:0.04) $KH_2PO_4-Na_2B_4O_7$ buffer, (C) 0.14 M (1.0:4.3) $Na_2SiF_6-Na_2B_4O_7$ buffer, (D) 5.0×10^{-2} M (1.0:1.3) $Na_2SiF_6-NaHCO_3$ buffer. The concentration of $[Ru(bpy)_3]^{2+}$ was 1.1×10^{-4} M. Initial and final pH values are given at the end of the curves. Dashed line indicates the theoretical turnover number for complete consumption of the $S_2O_8^{2-}$ sacrificial acceptor.

and pH dependent. More detailed studies (beyond the scope of this paper) will be needed to determine if the initial steps in the decomposition are the same in the presence and absence of phosphate.

Reaction in Na_2SiF_6-Containing Buffers. To replace phosphate with another buffering ion of high capacity, we considered weakly nucleophilic and weakly coordinating inorganic anions. While there are several two-component or multicomponent buffers that are effective at pH 5, those containing organic bases are susceptible to oxidation by $[Ru(bpy)_3]^{3+}$. Figure 5 shows a titration curve of aqueous Na_2SiF_6, which is acidic because of partial hydrolysis to fluoride ions and silicic acid in water[15], with aqueous $Na_2B_4O_7$ ($pK_a = 9.2$). The titration curve has a broad plateau at pH 5−6, indicating that Na_2SiF_6 solutions are effective buffers in this range. In addition, Na_2SiF_6 and its hydrolysis products are very weak nucleophiles and electrochemically stable over the relevant range of solution potentials.

Time courses of O_2 evolution and turnover numbers of the photosensitizer in two SiF_6^{2-}-containing buffers are compared in Figure 6 to phosphate-buffered and unbuffered solutions. In each case, the amount of base ($Na_2B_4O_7$ or $NaHCO_3$) added

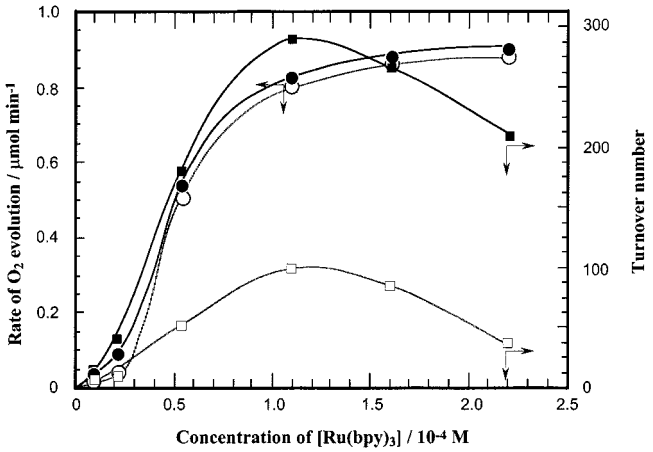

Figure 7. Dependence of the rate of O_2 evolution and turnover number on the concentration of $[Ru(bpy)_3]^{2+}$. Closed circles and squares represent the rate of O_2 evolution and turnover number in 5.0×10^{-2} M $Na_2SiF_6-NaHCO_3$ buffer, respectively. Open circles and squares represent the rate of O_2 evolution and turnover number in 0.14 M Na_2SiF_6- $Na_2B_4O_7$ buffer, respectively.

was sufficient to reach an initial pH of 5.4−5.5. Na_2SiF_6 buffers were more effective in maintaining the pH above 5 and improved the turnover number. The turnover number in the $Na_2SiF_6-Na_2B_4O_7$ buffer reached 100, i.e., twice that obtained under optimized conditions in $KH_2PO_4-Na_2B_4O_7$. In the case of the $Na_2SiF_6-NaHCO_3$ buffer, 25 μmol of O_2 was evolved without any decrease in activity. This value corresponds closely to the amount of O_2 that can be evolved by stoichiometric reduction of the sacrificial donor. A subsequent reaction was performed by adding 50 μmol of $Na_2S_2O_8$ and then sufficient $NaHCO_3$ to restore the pH to 5.4. The rate of O_2 evolution was about half that of the first reaction, and 15 μmol of O_2 was evolved. The lower rate in the second photolysis reaction can be attributed to the fact that about 50−60% of the sensitizer was decomposed in the first reaction. The total turnover number obtained from the first and second reactions was 290, substantially more than the best previously achieved (80) in the optimized $[Ru(bpy)_3]^{2+}-RuO_2$ system.[7] The O_2 yield of $[Ru(bpy)_3]^{2+}$−colloidal IrO_2 system has been reported to be considerably less than that of the former system.[9]

From Figure 6, the quantum efficiencies for O_2 evolution in 1.1×10^{-2} M $KH_2PO_4-Na_2B_4O_7$, $Na_2SiF_6-Na_2B_4O_7$, and $Na_2SiF_6-NaHCO_3$ buffers were estimated to be ca. 50% in the early stages of reaction (5−10 min). The decomposition rate constants of $[Ru(bpy)_3]^{3+}$ without colloidal IrO_2 in various buffers are summarized in Table 1. The rate constants for decomposition in no buffer, 1.1×10^{-2} M $KH_2PO_4-Na_2B_4O_7$, $Na_2SiF_6-Na_2B_4O_7$, and $Na_2SiF_6-NaHCO_3$ are the same within experimental error. This suggests two possibilities for the better performance of the system in $Na_2SiF_6-Na_2B_4O_7$ and $Na_2SiF_6-NaHCO_3$ buffers. One is that the improvement arises from an increased rate of reduction of $[Ru(bpy)_3]^{3+}$ to $[Ru(bpy)_3]^{2+}$ at the surface of the colloid, or from a subsequent rate determining step in O_2 evolution from the colloid, since the background decomposition rates are the same. The second possibility is that oxidized sensitizer molecules adsorbed on the surface of the IrO_2 colloid are decomposed faster than those in the bulk solution, except in the presence of bicarbonate. Several additional experiments were carried out to determine that the latter explanation is in fact the correct one.

Figure 7 shows the dependence of the turnover number and O_2 evolution rate on the concentration of photosensitizer in the $Na_2SiF_6-Na_2B_4O_7$ and $Na_2SiF_6-NaHCO_3$ buffers. In cases

where the sacrificial acceptor was completely consumed by O_2 evolution, the reaction was resumed after 50 μmol of $Na_2S_2O_8$ was added and the pH was restored to its initial value by addition of the appropriate base ($Na_2B_4O_7$ or $NaHCO_3$). The rate of O_2 evolution plotted in this figure is that observed in the early stages of the reaction (<10 min), before significant decomposition of the oxidized sensitizer occurs.

Interestingly, the initial oxygen evolution rates are virtually identical for the two buffer systems, and both have the same sigmoidal shape. The coincidence of these initial rate curves argues strongly that the effect of bicarbonate is not to accelerate interfacial electron transfer or oxygen evolution reactions, since those (if they were rate determining) would also affect the initial rate. The initial rate curve saturates in the manner of an adsorption isotherm, suggesting that oxygen evolution occurs only when sensitizer molecules are adsorbed on the colloid. The fact that the turnover rates are low at low concentration is consistent with this idea; that is, at low concentration, a larger fraction of the sensitizer is free in solution and subject to decomposition, because it cannot be reduced by the colloid. The entire initial rate curve resembles a Langmuir isotherm, except that it has upward curvature at low concentration. At the lowest sensitizer concentrations, oxygen evolution is not observed in the first 5 min of the reaction, but is observed after this induction period. Hence, the points measured at very low concentration do not truly represent a steady-state initial rate.

In both buffers, the turnover number reaches a maximum as the rate of O_2 evolution reaches a plateau at ca. 1.1×10^{-4} M. Under photochemical conditions, most of the photosensitizer is present as $[Ru(bpy)_3]^{3+}$, as noted above. Beyond 1.1×10^{-4} M concentration, the background decomposition rate exceeds the rate of oxygen evolution and the turnover number decreases. It is significant that the initial rate curves reach a plateau rather than a maximum in Figure 7. This means that electrons are exchanged between adsorbed and nonadsorbed sensitizer molecules (or, the molecules themselves exchange at the colloid surface). Otherwise, excess sensitizer molecules in solution would create an "inner filter" effect and the rate of oxygen evolution would decrease with increasing concentration, because a smaller fraction of the light is absorbed by colloid-adsorbed sensitizer molecules.

Effect of Bicarbonate and Borate on the IrO_2 Colloid. As noted above, there is no significant difference in background decomposition rates of $[Ru(bpy)_3]^{3+}$, or in initial oxygen evolution rates, in $Na_2SiF_6-Na_2B_4O_7$ and $Na_2SiF_6-NaHCO_3$ buffers. However, the turnover number in the $Na_2SiF_6-NaHCO_3$ buffer is about 3 times larger than that in $Na_2SiF_6-Na_2B_4O_7$. Apparently, the higher turnover number in $Na_2SiF_6-NaHCO_3$ can be attributed to bicarbonate ions and their effect on the surface chemistry of the IrO_2 colloid.

One possible effect of bicarbonate ions might be to cause the cationic sensitizer to adsorb more strongly to the surface of the colloid. To estimate the amount of adsorbed photosensitizer on the colloid, the IrO_2 particles were attached to amine-derivatized silica. Amine-derivatized silica can adsorb colloidal IrO_2 particles because the latter possess a negative surface charge at pH > 2.[5] The preparation of amine-derivatized silica has been described elswhere.[13] A portion, 0.1 g, of amine-derivatized silica was stirred for 1 h in 80 mL of 6.2×10^{-4} M colloidal IrO_2. The amount of adsorbed colloid was estimated to be 5.0×10^{-4} mol/g from UV−vis spectra of a colloidal IrO_2 solution (which has a broad absorption band between 500 and 700 nm[8]) before and after adsorption. Portions of the colloidal IrO_2/amine/silica composite (0.01 g) were stirred vigorously in 5 mL each of 1.1×10^{-4} M $KH_2PO_4-Na_2B_4O_7$, $Na_2SiF_6-Na_2B_4O_7$, and $Na_2SiF_6-NaHCO_3$ buffers containing the optimum concentration (1.1×10^{-4} M) of $[Ru(bpy)_3]^{2+}$ (5.5×10^{-7} mol). Each solution was adjusted to pH 5.7. After stirring for 5 h, the suspensions were centrifuged. The adsorbed amounts of $[Ru(bpy)_3]^{2+}$ in $KH_2PO_4-Na_2B_4O_7$, $Na_2SiF_6-Na_2B_4O_7$, and $Na_2SiF_6-NaHCO_3$ buffers were 1.3×10^{-7}, 1.6×10^{-7}, and 1.2×10^{-7} mol, respectively, as determined by UV−vis spectroscopy of the supernatants. $[Ru(bpy)_3]^{2+}$ was not adsorbed on amine-derivatized silica without colloidal IrO_2. In each case the quantity of $[Ru(bpy)_3]^{2+}$ adsorbed corresponds approximately to saturation coverage of the colloid (ca. 10^{-10} mol/cm^2, from the size of the colloidal particles in Figure 1). This argues that the increased turnover number in $Na_2SiF_6-NaHCO_3$ buffer cannot be attributed simply to an increase in the amount of adsorbed sensitizer.

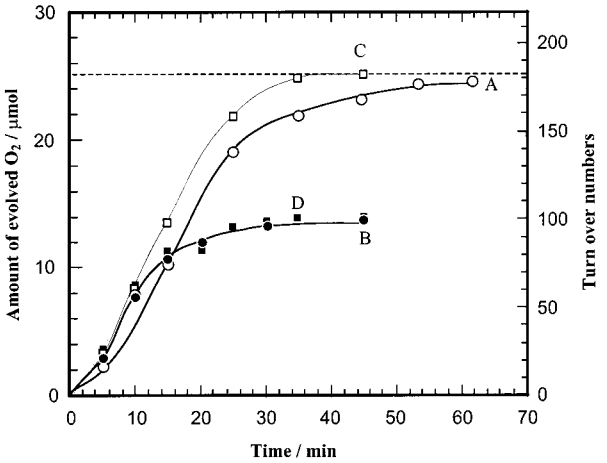

Figure 8. Time course of O_2 evolution and turnover number in 0.14 M $Na_2SiF_6-Na_2B_4O_7$ buffer containing $NaHCO_3$. (A), (B) 0.14 M $Na_2SiF_6-Na_2B_4O_7$ buffer containing 1.2×10^{-3} M $NaHCO_3$ (see text); (C) 5.0×10^{-2} M $Na_2SiF_6-NaHCO_3$ buffer; (D) in 0.14 M $Na_2SiF_6-Na_2B_4O_7$ buffer.

A further test of the effect of bicarbonate ions was made by adding bicarbonate to the borate buffer. Figure 8 shows the time course of O_2 evolution in 0.14 M $Na_2SiF_6-Na_2B_4O_7$ buffer containing 1.2×10^{-3} M $NaHCO_3$. The concentrations of $[Ru(bpy)_3]^{3+}$, colloidal IrO_2, $Na_2S_2O_8$, and Na_2SO_4 were 1.1×10^{-4}, 6.2×10^{-5}, 1.1×10^{-2}, and 5.0×10^{-2} M, as before. Solution A was prepared from a colloidal IrO_2 solution obtained by dissolving 1.4×10^{-3} mol $NaHCO_3$ in 100 mL of 6.2×10^{-4} M colloidal IrO_2 solution, followed by stirring for 12 h and adding the other components. In the case of solution B, $NaHCO_3$ was added to the reaction solution prepared with $Na_2SiF_6-Na_2B_4O_7$ as described above. Time courses of O_2 evolution for $Na_2SiF_6-NaHCO_3$ (C) and $Na_2SiF_6-Na_2B_4O_7$ (D) buffers are also shown for comparison. The time course of the reaction of solution A, in which bicarbonate was added first, resembles that of the $Na_2SiF_6-NaHCO_3$ buffer, whereas that of solution B is almost identical to that of the $Na_2SiF_6-Na_2B_4O_7$ buffer. The substantial difference between traces A and B shows that bicarbonate does not simply displace borate from the surface of the colloid; rather, the adsorption of at least one of these anions must be irreversible or must cause an irreversible structural change in the colloid surface.

Arakawa et al. reported that photocatalytic overall water splitting proceeds on platinum-loaded TiO_2 particles in water in the presence of excess carbonate.[16,17] In general, it is difficult for a catalyst dispersed in water to evolve H_2 and O_2 simultaneously because of the exoergic reverse reaction on platinum

($2H_2 + O_2 \rightarrow 2H_2O$) and the difficulty of desorbing O_2 from the TiO_2 surface. Apparently, excess carbonate facilitates the desorption of O_2, preventing the reverse reaction in this photocatalytic system. Although the details of the reaction mechanism have not been determined, it seems that the formation of carbonate peroxides and photodecomposition of these peroxides contribute to the reaction, because water splitting proceeds only with light of much shorter wavelength than the band gap of TiO_2 ($E_g = 3$ eV, $\lambda = 410$ nm).[18] It is unlikely that such a mechanism can be operative in the sensitized IrO_2 system, since the reaction proceeds efficiently in visible light.

To summarize the foregoing results, there is no significant difference in the rate of O_2 evolution in the early stages of reaction between $Na_2SiF_6-Na_2B_4O_7$ and $Na_2SiF_6-NaHCO_3$ buffers, even though the turnover number is much greater in the latter. The remaining possible explanation for the difference is that adsorbed borate and phosphate ions increase the decomposition rate of oxidized sensitizer molecules that are adsorbed to the colloid surface, whereas bicarbonate does not. In the case of borate, the maximum turnover number is ca. 100. From the corresponding initial rate of oxygen evolution (see Figure 7), the quantum yield (ca. 50%), and the stoichiometry of the reaction (four turnovers per O_2), we can estimate the background decomposition rate to be ca. 1×10^{-2} s^{-1}, almost a factor of 10 higher than it is in the absence of the colloid. In the bicarbonate system, the turnover number is three times higher and the background decomposition rate is 3×10^{-3} s^{-1}, comparable to that in the colloid-free buffered or unbuffered solutions.

Conclusions

In the photocatalytic oxidation of water by the $[Ru(bpy)_3]^{2+}-$colloidal IrO_2 system, the lifetime and turnover number of the photosensitizer depend strongly on the choice of buffer. Because the system operates best at ca. pH 5, inorganic buffers with pK_a values in this range are needed. The previously studied phosphate−borate buffer promotes the decomposition of the oxidized sensitizer at the high concentrations needed to fix the pH, and the optimized turnover number is relatively small. Na_2SiF_6−borate and Na_2SiF_6−bicarbonate buffers control the pH and, in homogeneous solution, do not increase the background decomposition rate of $[Ru(bpy)_3]^{3+}$. However, at the optimum concentration of $[Ru(bpy)_3]^{2+}$, the surface of the colloid is completely covered by sensitizer molecules, and under these conditions it is the decomposition rate of adsorbed $[Ru(bpy)_3]^{3+}$ that determines the turnover number. Under these conditions, the $Na_2SiF_6-NaHCO_3$ buffer is most effective.

These results suggest that the maximum turnover rate per photosensitizer molecule, ca. 0.2 s^{-1} in the most optimized oxygen evolution system, is quite low. It was established by varying the intensity of the light source between 4 and 18 mW/cm^2 that, in the optimized system, the initial O_2 evolution rate was power-insensitive. Because oxidative quenching of the MLCT state $[Ru(bpy)_3]^{2+}$ by persulfate is fast, this means that the rate-determining step in the process must be one of the dark reactions, such as electron transfer between the colloid and $[Ru(bpy)_3]^{3+}$, charge transport within the colloidal particles, or oxygen evolution. Thus, while carbonate-modified colloidal IrO_2 catalysts with adsorbed sensitizer molecules may be a useful building block for complex nanoscale systems that are designed to perform overall water splitting, such systems will need to have especially low rates of back electron transfer in order to operate efficiently. Experiments designed to optimize these rates, to determine the rate-determining step in the IrO_2 catalyst system, and to investigate other colloids with possibly faster oxygen evolution kinetics are clearly needed and will be the subject of future work.

Acknowledgment. This work was supported by the Division of Chemical Sciences, Office of Basic Energy Sciences, Department of Energy, under contract DE-FG02-93ER14374. We thank Dr. Rosemary Walsh and the Electron Microscope Facility for the Life Sciences in the Biotechnology Institute at Pennsylvania State University for the use of the transmission electron microscope.

References and Notes

(1) (a) Ikeda, S.; Takata, T.; Kondo, T.; Hitoki, G.; Hara, M.; Kondo, J. N.; Domen, K.; Hosono, H.; Kawazoe, H.; Tanaka, A. *J. Chem. Soc., Chem. Commun.* **1998**, 2185. (b) Domen, K. *Catal. Today* **1998**, *44*, 17.

(2) Khaselev, O.; Turner, J. A. *Science* **1998**, *280*, 425.

(3) (a) Kudo, A.; Kato, H.; Nakagawa, S. *J. Phys. Chem. B* **2000**, *104*, 571. (b) Kim, H. G.; Hwang, D. W.; Kim, J.; Kim, Y. G.; Lee, J. S. *J. Chem. Soc., Chem. Commun.* **1999**, 1077.

(4) Limburg, J.; Vrettos, J. S.; Liable-Sands, L. M.; Rheingold, A. L.; Crabtree, R. H.; Brudvig, G. V. *Science* **1999**, *283*, 1524.

(5) Kiwi, J.; Grätzel, M. *Nature* **1979**, 285, 657.

(6) Kiwi, J.; Grätzel, M. *J. Am. Chem. Soc.* **1979**, *101*, 7214.

(7) Harriman, A.; Richoux, M.; Christensen, P. A.; Moseri, S.; Neta, P. *J. Chem. Soc., Faraday Trans. 1* **1987**, *83*, 3001.

(8) Harriman, A.; Thomas, J. M.; Millward, G. R. *New J. Chem.* **1987**, *11*, 757.

(9) Harriman, A.; Pickering, I. J.; Thomas, J. M.; Christensen, P. A. *J. Chem. Soc., Faraday Trans. 1* **1988**, *84*, 2795.

(10) Ghosh, P. K.; Brunschwig, B. S.; Chou, M.; Creutz, C.; Sutin, N. *J. Am. Chem. Soc.* **1984**, *106*, 4772.

(11) Dutta, P. K.; Das, S. K. *J. Am. Chem. Soc.* **1997**, *119*, 4311.

(12) Kaschak, D. M.; Mallouk, T. E. *J. Am. Chem. Soc.* **1996**, *118*, 4222.

(13) Kerimo, J.; Adams, D. M.; Barbara, P. F.; Kaschak, D. M.; Mallouk, T. E. *J. Phys. Chem.* B **1998**, *102*, 9451.

(14) Kaschak, D. M.; Lean, J. T.; Waraksa, C. C.; Saupe, G. B.; Mallouk, T. E. *J. Am. Chem. Soc.* **1999**, *121*, 3435.

(15) Mellor, J. W. *A Comprehensive Treatise on Inorganic and Theoretical Chemistry*; Longmans, Green & Co.: New York, 1925; Vol. 6, p 943.

(16) Sayama, K.; Arakawa, H. *J. Chem. Soc., Chem. Commun.* **1992**, 150.

(17) Sayama, K.; Arakawa, H. *Chem. Lett.* **1992**, 253.

(18) Sayama, K.; Arakawa, H. *Syokubai* **1993**, *35*, 142.